Sensors and Actuators B 209 (2015) 486–489

Contents lists available at ScienceDirect

Sensors and Actuators B: Chemical

journal homepage: www.elsevier.com/locate/snb

Short communication

Sensitivity and detection limit analysis of silicon nanowire bio(chemical) sensors

Songyue Chen[a,*], Albert van den Berg[a], Edwin T. Carlen[a,b,**]

[a] MESA+ Institute for Nanotechnology & MIRA Biomedical Technology and Technical Medicine, University of Twente, 7522 NH Enschede, The Netherlands
[b] Graduate School of Pure and Applied Science, University of Tsukuba, 305-8573 Tsukuba, Japan

ARTICLE INFO

Article history:
Received 31 July 2014
Received in revised form 20 November 2014
Accepted 2 December 2014
Available online 10 December 2014

Keywords:
Silicon nanowire
Sensitivity
Detection limit
Signal to noise ratio

ABSTRACT

This paper presents an analysis of the sensitivity and detection limit of silicon nanowire biosensors using an analytical model in combination with *I–V* and current noise measurements. The analysis shows that the limit of detection (LOD) and signal to noise ratio (SNR) can be optimized by determining an operating point in the depletion region with a large sensor transconductance, while maintaining a small system output noise amplitude. Both sensor and measurement configurations play equally important roles for optimal sensor performance. The analysis also shows that the LOD and SNR are minimally affected by the sensor cross-sectional geometry and size.

1. Introduction

With the rising popularity of silicon nanowire (Si-NW) field-effect (FET) biosensors, understanding their physical behavior is important for systematically improving their sensitivity and limit of detection (LOD). Si-NW FET sensors are different than their planar predecessors [1] due to their nanoscale three-dimensional geometry, which is important for chemical and biochemical sensors. The three-dimensional geometry provides a multi-gate interface with a large surface area to volume ratio, which can render them extremely sensitive to the binding of small quantities of target species on the sensor surface [2–4]. Additionally, the nanoscale multi-gate sensing surface requires a smaller number of molecules to generate the same gate potential change compared to the macroscale planar sensors.

A typical Si-NW biosensor system is comprised of a multi-gate Si-NW FET biosensor, reference electrode and power supply (V_{fg}) for front-gate control (fg), power supply (V_{bg}) for back-gate (bg) control, power supply (V_{ds}) for the NW bias current control, and a current measurement instrument (I), as shown in Fig. 1(a). Multi-gate Si-NW FET biosensors are usually configured in a dual gate configuration, indicated as fg and bg in Fig. 1(a). The bg controls the back gating of the sensor body, and the fg controls the front gating of the upper sensor surface in contact with the electrolyte solution. Surface reactions at the gate-oxide surface, due to electrolyte ions, or the binding of charged target molecules, result in a change in the surface charge density $\Delta\sigma$ and subsequent surface potential change $\Delta\psi_o$, which induce a change in the Si-NW current ΔI. The majority of Si-NW FET biosensors use a p-type doped body and the operating region of the depletion-mode devices depends on the body doping and the bias voltages V_{fg} and V_{bg}.

Fig. 1(b) shows typical *I–V* curves from depletion-mode Si-NW sensors with triangular cross-section (length 7 μm, height 100 nm), developed by our research group, and measured in a 0.1 M NaCl supporting electrolyte with a 10 mM universal buffer mixture (10 mM citric acid, 10 mM phosphoric acid, and 20 mM boric acid, pH 7.0) using a reference electrode (REF200, Ag/AgCl, Radiometer Analytical) for liquid gating. In these measurements, the sensor current I is measured with a lock-in amplifier instrument (SR830, Stanford Research Systems), however, a DC power source for V_{ds} is used for the rest of the noise measurements unless mentioned specifically. Four different operation regions are indicated in the measured *I–V* curves. For $V_T \le V_{fg} \le V_{off}$, where V_{off} is the pinch-off voltage and V_T is the threshold voltage (Fig. 1(b), inset), the devices operate in the weak current region, sometimes referred to as a subthreshold region [5]. For $V_{fb} \le V_{fg} \le V_T$, where V_{fb} is the applied gate voltage necessary to induce a flat energy band at the

* Corresponding author. Tel.: +31 53489 4851.
** Corresponding author at: Graduate School of Pure and Applied Science, University of Tsukuba, 305-8573 Tsukuba, Japan.
E-mail addresses: s.chen@utwente.nl (S. Chen), ecarlen@ims.tsukuba.ac.jp (E.T. Carlen).

http://dx.doi.org/10.1016/j.snb.2014.12.007
0925-4005/

silicon surface, the current decreases from the non-depleted flat-band condition ($V_{fg} = V_{fb}$). For $V_{fg} < V_{fb}$, the total device current is due to a combination of the majority carriers in the device body and the accumulation surface layer.

2. Methodology

We previously reported an analytical model that describes the current of a Si-NW in the depletion and accumulation regions of operation [1]. The total current is the sum of the current of the device body and the accumulated majority carriers at the upper sensor surfaces $I = I_d + I_a$, which depends on the region of operation. The depletion current can be approximated with $I_d \approx q\mu_b V_{ds} N_a L^{-1} A_c(f_d, a)$, where q is the electronic charge, μ_b is the majority carrier mobility in the NW body, N_a is the NW body doping concentration, L is the length, a is the characteristic dimension of the NW cross-section (Fig. 1(c)), and f_d is a function that describes the two-dimensional depletion distance induced at the sensor surface due to surface potential change [1]. The depletion function can be approximated with $f_d \approx ((t_f\varepsilon_{Si}/\varepsilon_{ox})^2 + 2\varepsilon_{Si}(V_{fg} - V_{fb})/qN_a)^{1/2} - t_f\varepsilon_{Si}/\varepsilon_{ox}$, where ε_{Si} and ε_{ox} are the permittivity of silicon and silicon dioxide, respectively, and t_f is the gate-oxide thickness. The device current in the accumulation region I_a results from an accumulation layer of majority carriers induced at the surface of the NW [6]. The flat band voltage is $V_{fb} = \Gamma - \psi_o$, where the various surface potential terms are lumped into $\Gamma = E_{ref} - \phi_{Si}/q - Q_i/C_i - \chi^{sol} - \Delta\chi$, with E_{ref} is the potential drop due to the reference electrode, ϕ_{Si} is the silicon workfunction, Q_i and C_i represent the insulator effective charge per unit area and capacitance, χ^{sol} is the surface dipole potential, and $\Delta\chi$ represents various potential drops at the interface [7]. An applied V_{fg} compensates the potential drop Γ, due to the electrochemical system, and biases the sensor in a particular region of operation ($V_{fg} \equiv V_o$ and $I \equiv I_o$). This general relationship provides a direct connection between the sensor input ψ_o and output I, where changes in surface potential $\Delta\psi_o$ produce changes in the output as ΔI. Fig. 1(b) shows a comparison of the model (black open circles) and measured (solid blue line) data for a Si-NW with a triangular cross-section. In general, any NW cross-sectional geometry can be incorporated in the model (Fig. 1(c)) [8]. The main result of this analysis is that measurable current changes of the Si-NW sensors ΔI are generated by surface potential changes $\Delta\psi_o$; the surface potential changes are induced by changes in the surface charge density $\Delta\sigma$ due to binding of charged biomolecules, ion fluctuations, or solution pH variations.

In general, the sensitivity of a biosensor system, which consists of the sensor element and the measurement instrumentation, is defined as $Y \equiv \Delta F/\Delta M$, where F is the output response and M is the sensor input [9]. For Si-NW biosensors, surface potential changes $\Delta\psi_o$, due to the hybridization of charged target biomolecules to complementary probes attached directly to the sensing surface, induce ΔI. The system input is the target biomolecule concentration $[C]_a$. Each sample concentration $[C]_a$ will induce a $\Delta\psi_{o,a}$, and therefore, we define $\psi_a \equiv \Delta\psi_{o,a}$ to represent the surface potential change at each sample concentration. For biochemical sensors, ion concentration and pH gradients also produce surface potential changes that are proportional to $[C]_a$. Therefore, we use I as the system output and ψ_a as the system input for both chemical and biological Si-NW sensor systems. The sensitivity is then defined as $Y \equiv \Delta I/\Delta\psi_a$, since each target concentration $[C]_a$ results in an independent surface charge change $\Delta\psi_a$. It should be noted that for a certain $[C]_a$, the surface potential change is also dependent on the ionic strength and pH of the background electrolyte [10]. For a single sensor measurement configuration, $I = I_o + \Delta I$, where I_o is the sensor bias current and ΔI is the sensor response induced by $\Delta\psi_{o,a}$ for a particular sample concentration $[C]_a$ [11]. The resolution of the measurement of ΔI is dependent on the magnitude of I_o; for large

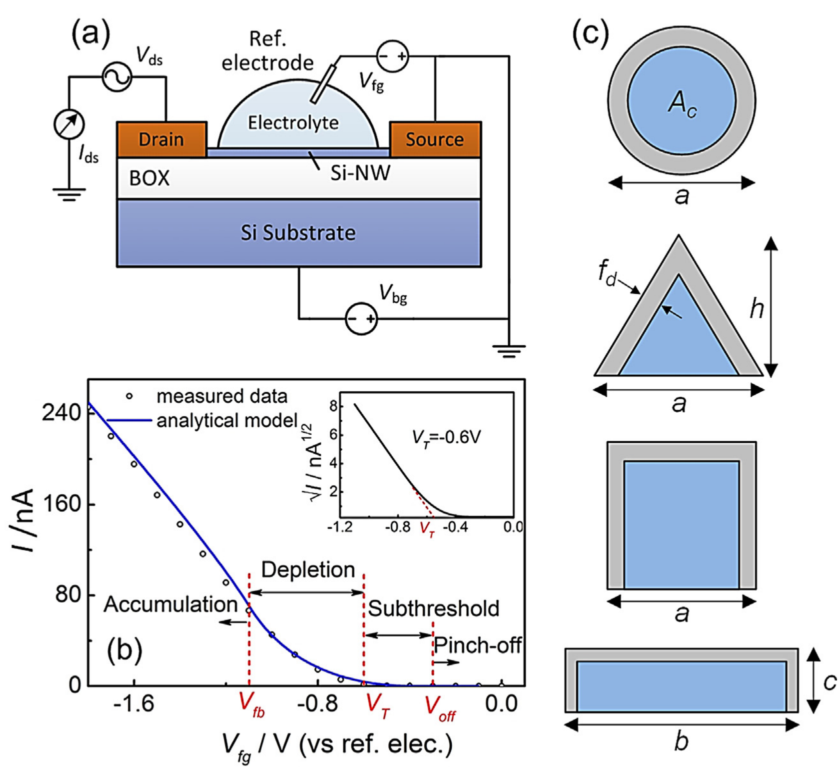

Fig. 1. (a) Si-NW biosensor biasing and measurement configurations, (b) measured (open circles) and modeled (solid line) I–V curves showing the operation regions of a typical depletion-mode Si-NW biosensor with $V_{ds} = 0.1$ V and $V_{bg} = 0$ V, (c) common Si-NW cross-section shapes: circular, triangular, square, and ribbon; and their characteristic dimensions, heights h and c, base width a, conductance area A_c (blue regions), and depletion distance f_d at the sensor surface (gray depletion regions). (For interpretation of the references to color in this figure legend, the reader is referred to the web version of this article.)